

Neuro-flow Dynamics and the Learning Processes

M. TATSUNO and Y. AIZAWA

Department of Applied Physics, School of Science and Engineering
Waseda University, Shinjuku, Tokyo 169, JAPAN

Abstract – A new description of the neural activity is introduced by the neuro-flow dynamics and the extended Hebb rule. The remarkable characteristics of the neuro-flow dynamics, such as the primacy and the recency effect during awakesness or sleep, are pointed out.

(Accepted 2 December 1996)

1. INTRODUCTION

Research of the central nervous systems has attracted much attention recently, and a large number of contributions, especially theoretical ones, have been made by physicists since the 1980's [1, 2, 3]. In these researches, theoreticians have made very simplified models of the brain, and studied their statistical properties analytically as well as numerically. Among those models, the Hopfield model and its extensions have been thoroughly studied, and many interesting properties have been obtained, including the famous $p/N \approx 0.14$ limit where N is the number of neurons and p is the number of stored patterns [2, 4]. An important hypothesis generally used on these models is the Hebb rule, that is to say, “the changes of synaptic strength are proportional to the correlation between the firing of the pre- and post-synaptic neurons” [5]. The original idea by Hebb has been changed a little, i.e., firing of the post-synaptic neuron is not always necessary and the change of the membrane potential is more significant for synaptic plasticity [6, 7]. However there still remain many problems in the molecular process of synaptic transmission. The molecular basis of the Hebb rule has been pursued precisely to explain synaptic activity [7].

Many qualitative behaviors of neural networks have been elucidated based on the Hebb rule mentioned above, but there still remain many differences between the real functions of the brain and artificial neural networks. The most important of them is that the real brain always works in the non-equilibrium states accompanied by nerve impulses. On the other hand, models of artificial neural networks have been treated in the equilibrium state of the thermo-dynamical limit. Thus, it is inevitable that the model of neural networks is extended to the non-equilibrium state. In this paper, we will propose a new model of neuro-flow dynamics in which the essential variable to describe the neural activity is the flow rate of neuro-impulses which propagate from the j th to the i th neuron. Furthermore, the original Hebb rule should be extended to include synaptic plasticity due to the neural flow. In this paper we will discuss some remarkable effects generated by the neuro-flow dynamics with the extended Hebb rule.

2. MODEL OF NEURO-FLOW DYNAMICS

The standard representation of neural networks in discrete time is written by

$$\sigma_i(t+1) = f_T\left(\sum_{j=1}^N w_{ij}(t)\sigma_j(t) - h_i\right) \quad (1)$$

where σ_i and h_i are the neuronal activity and the threshold of the i th neuron respectively, w_{ij} is the element of the connection matrix which stands for the coupling strength from the j th to the i th neuron and $f_T(\cdot)$ is a monotonically increasing function ($0 \leq f_T(\cdot) \leq 1$) with a parameter T . Multiplying $w_{ki}(t+1)$ to both sides of equation (1) and introducing a new variable $Y_{ki}(t) = w_{ki}(t)\sigma_i(t)$, equation (1) can be rewritten as

$$Y_{ki}(t+1) = w_{ki}(t+1)f_T\left(\sum_{j=1}^N Y_{ij}(t) - h_i\right). \quad (2)$$

Here Y_{ij} describes the flow rate of impulse transmission from the j th to the i th neuron. The variable Y_{ij} represents the strength of the impulse flow qualitatively and equation (2) describes the essential effect of the neuro-flow, but the dynamics of the flow variable Y_{ij} given by equation (2) cannot be uniquely determined. In order to recover the deterministic equation of the flow variable Y_{ij} , let us replace the

term $w_{ki}(t+1)$ by $w_{ki}(t)$ in equation (2). Thus, the Markovian equation of the flow variable X_{ij} instead of Y_{ij} is obtained

$$X_{ki}(t+1) = w_{ki}(t)f_T\left(\sum_{j=1}^N X_{ij}(t) - h_i\right). \quad (3)$$

Since our purpose is to elucidate the effect of the neuro-flow, both equation (2) and equation (3) should be the starting point for that purpose. But from the view point of the consistent description of the system, we consider that equation (3) is more natural than equation (2). For the sake of simplicity, the dynamics described by equation (1) is called the pattern dynamics, on the other hand, the dynamics given by equation (3) is known as the neuro-flow dynamics in this paper. We rewrite equation (3) using $X_{ki}(t) = w_{ki}(t-1)\sigma_i(t)$, the pattern dynamics of the variable σ_i corresponding to equation (3) can be given by

$$\sigma_i(t+1) = f_T\left(\sum_{j=1}^N w_{ij}(t-1)\sigma_j(t) - h_i\right). \quad (4)$$

This explains the essential difference between equations (1) and (4), that is to say, equation (1) is simple Markovian, but equation (4) is not. Thus, the flow dynamics of equation (3) can be expected to reveal quite complex aspects in comparison with the pattern dynamics of equation (1). To summarize, the neuro-flow dynamics, introduced by equation (3), is equivalent to the pattern dynamics with time-delayed effects.

3. EXTENSION OF THE HEBB RULE

The Hebb rule is often written by

$$w_{ij}(t+1) = Aw_{ij}(t) + C(2\zeta_i^\mu - 1)(2\zeta_j^\mu - 1) \quad (5)$$

where A is the decreasing rate C is the learning acquisition rate, and the second term of the right hand side stands for the learning term generated by the learning patterns $\{\zeta_i^\mu\}$ ($\zeta_i^\mu = 1$ or 0 with equal probability and $\mu = 1, \dots, p$). To store the learning patterns as local minima, the learning term $2\zeta_i^\mu - 1$ is used instead of ζ_i^μ . Here we rewrite $\xi_i^\mu = 2\zeta_i^\mu - 1$ and extend equation (5) by taking account the flow effect as follows

$$w_{ij}(t+1) = Aw_{ij}(t) + BX_{ij}(t+1) + C\xi_i^\mu \xi_j^\mu. \quad (6)$$

In this paper, we only discuss the case of $B > 0$ according to the original Hebb's idea. equation (6) is the simplest extension which introduces the flow effect of the nerve transmission.

Dynamical systems given by equations (3) and (6) can be solved by iteration. Let us show the solution for the special case $h_i = 0$, where the initial condition is given by $w_{ij}(0) = 0$, $X_{ij}(0) = 0$ and $f_T(\cdot)$ is a monotonically increasing function satisfying $f_T(0) = 1/2$, $f_T(+\infty) = 1$ and $f_T(-\infty) = 0$. The first two steps in the time course can be obtained

$$\begin{aligned} X_{ki}(1) &= w_{ki}(0)f_T\left(\sum_{j=1}^N X_{ij}(0)\right) \\ &= 0 \\ w_{ki}(1) &= Aw_{ki}(0) + BX_{ki}(1) + C\xi_k^1 \xi_i^1 \\ &= C\xi_k^1 \xi_i^1, \end{aligned} \quad (7)$$

$$\begin{aligned} X_{ki}(2) &= w_{ki}(1)f_T\left(\sum_{j=1}^N X_{ij}(1)\right) \\ &= \frac{C}{2}\xi_k^1 \xi_i^1 \\ w_{ki}(2) &= Aw_{ki}(1) + BX_{ki}(2) + C\xi_k^2 \xi_i^2 \\ &= C\left\{\left(A + \frac{B}{2}\right)\xi_k^1 \xi_i^1 + \xi_k^2 \xi_i^2\right\}. \end{aligned} \quad (8)$$

Here we consider two cases; One is the special case that the value ξ_i^μ of each pattern takes ± 1 randomly with the constraint $\sum_{j=1}^N \xi_j^\mu \rightarrow 0$ as $N \rightarrow \infty$ (Case 1). The other is the ordinary case where the value

ξ_i^μ takes ± 1 randomly, i.e. $\sum_{j=1}^N \xi_j^\mu \sim O(\sqrt{N})$ as $N \rightarrow \infty$ (Case 2).

3.1. Case 1

If we assume the value ξ_i^μ of each pattern takes ± 1 under the constraint that the pattern fluctuations are negligibly small in the limit of large system size N (i.e. $\sum_{j=1}^N \xi_j^\mu \rightarrow 0$ as $N \rightarrow \infty$), the solutions of equations (3) and (6) for the third time step can be analytically obtained

$$\begin{aligned}
X_{ki}(3) &= w_{ki}(2) f_T\left(\sum_{j=1}^N X_{ij}(2)\right) \\
&= C\left\{\left(A + \frac{B}{2}\right) \xi_k^1 \xi_i^1 + \xi_k^2 \xi_i^2\right\} f_T\left(\frac{C}{2} \xi_i^1 \sum_{j=1}^N \xi_j^1\right) \\
&= \frac{C}{2} \left\{\left(A + \frac{B}{2}\right) \xi_k^1 \xi_i^1 + \xi_k^2 \xi_i^2\right\} \\
w_{ki}(3) &= A w_{ki}(2) + B X_{ki}(3) + C \xi_k^3 \xi_i^3 \\
&= C\left\{\left(A + \frac{B}{2}\right)^2 \xi_k^1 \xi_i^1 + \left(A + \frac{B}{2}\right) \xi_k^2 \xi_i^2 + \xi_k^3 \xi_i^3\right\}.
\end{aligned} \tag{9}$$

After the iteration of p patterns, the solutions are

$$\begin{aligned}
X_{ki}(p) &= \frac{C}{2} \sum_{\mu=1}^{p-1} \left(A + \frac{B}{2}\right)^{(p-1)-\mu} \xi_k^\mu \xi_i^\mu \\
w_{ki}(p) &= C \sum_{\mu=1}^p \left(A + \frac{B}{2}\right)^{p-\mu} \xi_k^\mu \xi_i^\mu.
\end{aligned} \tag{10}$$

For the case of the normal Hebb rule (i.e. $B = 0$) the last few learning patterns ($\{\xi_i^\mu\}, \mu \approx p$) can be well stored due to the condition $A < 1$. But when the flow terms are introduced, i.e. $(A + B/2) > 1$, the first few learning patterns ($\{\xi_i^\mu\}, \mu \approx 1$) determine the connection matrix w_{ij} dominantly. As a result, the other learning patterns cannot be stably stored. We will explain this point later by numerical simulation.

3.2. Case 2

On the other hand, in the case of the more general condition where we assume that the value ξ_i^μ of each pattern takes ± 1 randomly, the solutions of equations (3) and (6) for the third time step change as follows:

$$\begin{aligned}
X_{ki}(3) &= w_{ki}(2) f_T\left(\sum_{j=1}^N X_{ij}(2)\right) \\
&= C\left\{\left(A + \frac{B}{2}\right) \xi_k^1 \xi_i^1 + \xi_k^2 \xi_i^2\right\} f_T\left(\frac{C}{2} \xi_i^1 \times \pm O(\sqrt{N})\right) \\
&= C\left\{\left(A + \frac{B}{2}\right) \xi_k^1 \xi_i^1 + \xi_k^2 \xi_i^2\right\} \frac{1 \pm \xi_i^1}{2} \\
w_{ki}(3) &= A w_{ki}(2) + B X_{ki}(3) + C \xi_k^3 \xi_i^3 \\
&= C\left\{\left(A + \frac{B}{2}\right) \xi_k^1 \xi_i^1 + \xi_k^2 \xi_i^2\right\} \left[A + \frac{B}{2} (1 \pm \xi_i^1)\right] + \xi_k^3 \xi_i^3.
\end{aligned} \tag{11}$$

After the iteration of p patterns, the solutions are

$$\begin{aligned}
X_{ki}(p) &= C\left\{\left(A + \frac{B}{2}\right) \xi_k^1 \xi_i^1 (\alpha_i^{\pm 1})^{p-3} + \sum_{\mu=2}^{p-1} (\alpha_i^{\pm 1})^{(p-1)-\mu} \xi_k^\mu \xi_i^\mu\right\} \frac{1 \pm \xi_i^1}{2} \\
w_{ki}(p) &= C\left\{\left(A + \frac{B}{2}\right) \xi_k^1 \xi_i^1 (\alpha_i^{\pm 1})^{p-2} + \sum_{\mu=2}^p (\alpha_i^{\pm 1})^{p-\mu} \xi_k^\mu \xi_i^\mu\right\}
\end{aligned} \tag{12}$$

where $\alpha_i^{\pm 1} = A + B(1 \pm \xi_i^1)/2$. Thus, in the case of the random learning patterns without constraints, the connection matrix is determined by $\alpha_i^{\pm 1}$ instead of $(A + B/2)$. For the case of the normal Hebb rule

($B = 0$), the last few learning patterns can be well stored since $A < 1$, and the matrix element $w_{ij}(p)$ of equation (12) becomes the same as that of equation (10). However, when $B > 0$, $\alpha_i^{\pm 1}$ takes $(A+B)$ or A . This implies that the last few learning patterns can be well stored for $(A+B) < 1$, but for $(A+B) > 1$ the first few learning patterns can be stored. We will explain this point later by numerical simulation.

4. SLEEP IN NEURO-FLOW DYNAMICS

Now let us further investigate equation (6) under the condition of no learning term, i.e. $C = 0$. When the external stimuli stop, the neural network evolves autonomously according to the neuro-flow dynamics equations (3) and (6) with $C = 0$. This situation can be compared with the state where the central nervous systems are sleeping, that is, the activity of brain is self-organized only by the internal information. The time evolution of w_{ij} during sleep can be written as

$$\begin{aligned} w_{ki}(t+1) &= Aw_{ki}(t) + BX_{ki}(t+1) \\ &= w_{ki}(t)[A + Bf_T(\sum_{j=1}^N X_{ij}(t) - h_i)]. \end{aligned} \quad (13)$$

In the case of the ordinary Hebb rule ($B = 0$), $w_{ij}(t)$ vanishes when $t \rightarrow \infty$ because of $A < 1$, but in the case of $B > 0$, $w_{ij}(t)$ does not always decrease. In other words, sleep in the neuro-flow dynamics brings about two quite different effects; one is forgetting of the memory, the other is reinforcement of the memory. The general criterion for forgetting or reinforcement is derived from equation (13):

$$\begin{aligned} w_{ki}(t+1) &\geq w_{ki}(t); & \text{for } f_T(\sum_{j=1}^N X_{ij}(t) - h_i) &\geq \frac{1-A}{B} \\ w_{ki}(t+1) &< w_{ki}(t); & \text{for } f_T(\sum_{j=1}^N X_{ij}(t) - h_i) &< \frac{1-A}{B}. \end{aligned} \quad (14)$$

We discuss the time evolution of $X_{ki}(t)$ and $w_{ki}(t)$ in the sleep condition for Case 1 and Case 2 as mentioned before.

4.1. Case 1

In the case of the random patterns with the constraint $\sum_{j=1}^N \xi_j^\mu \rightarrow 0$ as $N \rightarrow \infty$, after the learning obtained by equation (10) is finished, the addition of the l times sleep induces the following solutions:

$$\begin{aligned} X_{ki}(p+l) &= \frac{C}{2} \sum_{\mu=1}^p (A + \frac{B}{2})^{(p-1)+l-\mu} \xi_k^\mu \xi_i^\mu \\ w_{ki}(p+l) &= C \sum_{\mu=1}^p (A + \frac{B}{2})^{p+l-\mu} \xi_k^\mu \xi_i^\mu. \end{aligned} \quad (15)$$

Here in the case of $(A + B/2) > 1$, the matrix elements w_{ij} corresponding to the first few learning patterns can be much amplified after sleep. This is nothing but the reinforcement of the primacy effect [8] by sleep. On the other hand, every learning pattern is vanishing for $(A + B/2) < 1$.

4.2. Case 2

In the case of random patterns without constraints, the addition of the l times sleep after the learning of equation (12) induces the following solutions

$$\begin{aligned} X_{ki}(p+l) &= C \{ (A + \frac{B}{2}) \xi_k^1 \xi_i^1 (\alpha_i^{\pm 1})^{p+l-3} + \sum_{\mu=2}^{p-1} (\alpha_i^{\pm 1})^{(p-1)+l-\mu} \xi_k^\mu \xi_i^\mu \} \frac{1 \pm \xi_i^1}{2} \\ w_{ki}(p+l) &= C \{ (A + \frac{B}{2}) \xi_k^1 \xi_i^1 (\alpha_i^{\pm 1})^{p+l-2} + \sum_{\mu=2}^p (\alpha_i^{\pm 1})^{p+l-\mu} \xi_k^\mu \xi_i^\mu \}. \end{aligned} \quad (16)$$

Here every learning pattern will be erased for $\alpha_i^{\pm 1} < 1$, but the first few learning patterns can be amplified for $\alpha_i^{\pm 1} > 1$; the condition of the reinforcement of the primacy effect will be given by $(A + B) > 1$.

5. NUMERICAL SIMULATION

Let us now numerically investigate the neuro-flow dynamics with the extended Hebb rule. The values of the parameters used in this paper are fixed as follows: $N = 100$, $p = 10$, $h_i = 0$; the orthogonal learning patterns $\{\xi_i^\mu\}$ s are selected from the randomly produced patterns and they satisfy $\sum_{j=1}^N \xi_j^\mu \approx 0$ and $\sum_{j=1}^N \xi_j^\mu$ is set to 0 for Case 1. $f_T(x)$ is fixed as $f_T(x) = 1/(1 + \exp(-x/T))$ with $T = 0.05$. The time development is performed by the synchronous updating of equations (3) and (6) under the initial conditions of $w_{ij}(0) = 0$ and $X_{ij}(0) = 0$.

5.1. Case 1

The connection matrix $w_{ij}(p)$ were determined after the learning process mentioned above. The basin structure corresponding to the fixed matrix $w_{ij}(p)$ was searched by the Monte-Carlo simulations, i.e. initial values of the test flow $X_{ij}(0)$ s in equation (3) were distributed randomly in the range $-1 \leq X_{ij}(0) \leq 1$. The statistical properties of the basin structure can be represented by the rank-size relation of each pattern; the size is defined by the volume of the each basin and the rank of each basin is defined in accordance with the order of largeness of the basin volume. For example, rank 1 corresponds to the largest basin and rank 2 to the second largest basin, etc. Figure 1 shows the relation between rank n and the basin volume V for the case of $A = 1$ and $B = 0$. Here the filled circles stand for the learning patterns and the crosses for the spurious states. As is shown in Fig. 1, there exist a number of basins for spurious states and they obey

$$V \propto n^{-D} \quad (D = 0.5582152) \quad (17)$$

where D is the Zipf index. However all learning patterns have a larger basin volume than that of spurious states, and this clearly shows that the neuro-flow dynamics proposed here has the learning ability in the same level as the Hopfield model of neural networks. Furthermore, the rank-size relation obeys an inverse power law. This is also similar to the result that was reported in a previous paper treating the Hopfield model [9, 10].

When the flow term is introduced, the basin structure is drastically changed as is shown in Figs 2 and 3. Figure 2 reveals the flow effect on the learning process in the (A, B) parameter space. The number of stably stored learning patterns $M(M \leq p)$ is shown in the two-dimensional (A, B) parameter space in gray-scale. The axis of $B = 0$ corresponds to the case of the normal Hebb rule. All learning patterns are stably stored around $(A + B/2) = 1$ and the number of stably stored learning patterns M decreases almost monotonically as the distance from the line $(A + B/2) = 1$ increases. Figure 3 shows the change of the basin volume of each learning pattern ($\mu = 1, 2, \dots, 10$) for the various values of B at $A = 0.9$. We can see that when the value of B increases, the basin volume for the first few learning patterns ($\mu = 1, 2, 3$) become dominant for $B \gtrsim 0.2$ and the basin for spurious states gets smaller (to less than 10%). This result clearly reveals the primacy effect of the memory and is consistent with the theoretical prediction derived from equation (10). On the other hand, for the case of $B \lesssim 0.2$, the basin volume for the last few learning patterns ($\mu = 8, 9, 10$) become dominant. In other words, a transition occurs from the recency effect [8] to the primacy effect at the critical point $B \simeq 0.2$.

Next, further iteration after the learning ($p = 10$) by the neuro-flow dynamics without the learning term was performed numerically using equations (3) and (6) with $l = 1000$. Figures 4 and 5 show the results of the basin structures and the phase diagram. Comparing Fig. 4 with Fig. 2, one can see that memories are completely erased after sleep in the region of $(A + B/2) < 1$. Figure 5 shows the change of the basin volume for each learning pattern, where the value of parameter A is the same as in Fig. 3. The basin volume for the first few learning patterns ($\mu = 1, 2, 3$) increases much more sharply and the spurious basin becomes smaller very quickly for $B \geq 0.2$. On the other hand, in the case of $B < 0.2$, the basin volume for all learning patterns is vanishing. This shows that the primacy effect discussed in Fig. 3 is much more emphasized due to the sleep. Figure 5 appears to suggest that sleep reinforces and selects memories which were learned during awakesness, and that a lot of spurious memories are washed out during sleep. Actually the system approaches steady states after long sleep when the effects of the flow increases and the number of spurious memories becomes less than 10%.

5.2. Case 2

For the case of random patterns without constraints, the same numerical simulation was performed and quite different property was elucidated.

Figure 6 shows the relation between rank n and the basin volume V for the case of $A = 1$ and $B = 0$,

and spurious states obey

$$V \propto n^{-D} \quad (D = 0.5582152). \quad (18)$$

Here the learning ability of neuro-flow dynamics is clearly shown again by the fact that all the learning patterns have a larger basin volume than that of spurious states. As was expected from the theoretical analysis, the slope of Fig. 1 and that of Fig. 6 are completely same.

The flow effect on the learning process is shown in Fig. 7 and it is quite different from Fig. 2. The line $(A + B) = 1$ clearly separates two region: $(A + B) < 1$ and $(A + B) > 1$. In $(A + B) < 1$, all the learning patterns are stably stored at $A \approx 1$, in which $(A + B) \approx A$, and gradually decrease as A decreases. However, the number of stably stored patterns shows a complex structure depending on the combination of the value of $(A + B)$ and A . On the other hand, in $(A + B) > 1$ only one pattern is stored successfully, and this can be understood from equation (12). Since $\alpha_i^{\pm 1}$ takes $(A + B)$ or A according to the value ξ_i^1 and since $(A + B) > 1$ and $A < 1$, all the terms $\xi_k^\mu \xi_i^\mu$ ($\mu = 2, 3, \dots, p$) is totally disturbed and cannot be stably stored.

Figure 8 shows the change of the basin volume of each learning pattern for the various values of B at $A = 0.9$. We can clearly see the drastic change from the recency effect for $B \lesssim 0.1$ to the primacy effect for $B \gtrsim 0.1$ occurs. It is also surprising that all initial flows converge to the first learning pattern ($\mu = 1$) for $B > 0.1$ and all spurious states are washed out.

Next, the further iteration after learning ($p = 10$) was performed in the sleep condition with $l = 1000$. Figures 9 and 10 show the results of the basin structure and the phase diagram. As was seen in Fig. 4, the erasure of memories is also observed for $(A + B) < 1$ in Fig. 9. Figure 10 shows the change of the basin volume for each learning pattern, where the value of parameter A is the same as in Fig. 8. We can see that a much sharper change than Fig. 8 occurs at $B = 0.1$, that is, for $B < 0.1$ all learning patterns are erased, and for $B > 0.1$ the first learning pattern ($\mu = 1$) becomes dominant. It should be also pointed out that there are no spurious states in $B > 0.1$.

The above results indicate that sleep amplifies the primacy effect in the case of random patterns. Therefore, together with the results of Case 1, it can be suggested that sleep reinforces and selects the memories which were learned during awakesness, and that many spurious memories are erased during the sleep.

6. SUMMARY

We have proposed a neuro-flow dynamics with the extended Hebb rule to deal with the autonomy of the neural systems and have shown that the neuro-flow dynamics is equivalent to the pattern dynamics with a certain time delayed connection. Two essential new features are derived from the neuro-flow dynamics. One is the reinforcement of the primacy effect of the memory, the other is the striking effect of sleep which washes out the spurious memories. The latter point is quite similar to the idea that was mentioned by Click concerning the function of dreaming in sleep [11]. In this connection, the mechanism of the memory palimpsest, which was studied by Nadal et al. [12], in the future must be discussed in comparison with our neuro-flow dynamics model.

The analysis in this paper is only limited to the case only for random learning patterns and their special case. The extension to the non-random patterns will be discussed in a forthcoming paper together with the generalization of the neuro-flow dynamics model [13].

Acknowledgements – This work was partially supported by a Grant-in-Aid for Encouragement of Young Scientists from the Ministry of Education, Science and Culture. One of the authors (M. T.) appreciates the financial support of the Japan Society for the Promotion of Science for Japanese Junior Scientists.

References

- [1] J. Hopfield, Neural networks and physical systems with emergent collective computational abilities. Proc. Natl. Acad. Sci. USA **79**, 2554 – 2558 (1982).
- [2] D. J. Amit, H. Gutfreund and H. Sompolinsky, Strong infinite numbers of patterns in a spin-glass model of neural networks. Phys. Rev. Lett. **55**, 1530 – 1533 (1985); Statistical mechanics on neural networks near saturation. Ann. of Phys. **173**, 30 – 67 (1987).
- [3] J. Hertz, A. Krogh, R. G. Palmer, *Introduction to the Theory of Neural Computation*. Addison Wesley, Redwood (1991).
- [4] K. Tokita, The replica – symmetry – breaking solution of the Hopfield model at zero temperature: critical storage capacity and frozen field distribution. J. of Phys. A **27**, 4413 – 4424 (1994).
- [5] D. O. Hebb, *The Organization of Behavior*. Wiley, New York (1949).
- [6] T. P. V. Bliss and T. Lømo, Long – lasting potentiation of synaptic transmission in the dentate area of the anaesthetized rabbit following stimulation of the perforant path. J. Physiol. **232**, 331 – 356 (1973).
- [7] E. R. Kandel, J. H. Schwartz and T. M. Jessell, *Principles of Neural Science 3rd Edition*. Appleton & Lange, Norwalk (1991).
- [8] B. B. Murdock Jr, The serial position effect of free recall, J. Exp. Psychol. **64**, 482 – 488 (1962).
- [9] Y. Aizawa and K. Tokita, Zipf law in non-linear dynamics and neural nets. Proceedings of International Conference on Fuzzy Logic & Neural Networks IIZUKA '90 **2**, 637 – 640 (1990).
- [10] K. Arai and Y. Aizawa, Dynamical universality of neural networks – new aspects of basin structures –. Proceedings of the Second NOLTA Workshop on Nonlinear Dynamical Theory of Adaptively Learning Systems, 35 – 41 (1992).
- [11] F. Click and G. Mitchison, The function of dream sleep. Nature **304**, 111 – 114 (1983).
- [12] J. P. Nadal, G. Toulouse, J. P. Changeux and S. Dehaene, Networks of formal neurons and memory palimpsests. Europhys. Lett. **1**, 535 – 542 (1986).
- [13] M. Tatsuno and Y. Aizawa, in preparation.

Fig. 1. The rank-size relation of Case 1 for the basin volume obtained by Monte-Carlo simulation with 10000 randomly chosen initial conditions. The parameters are $A = 1.0$, $B = 0.0$ and $C = 1.0$. The filled circles correspond to the learning patterns and the crosses to spurious states. The solid line shows the fit of the spurious states by the least-squares method and the slope is -0.5582152 .

Fig. 2. Formation of the basin for the 10 random learning patterns with the constraint $\sum_{j=1}^N \xi_j^\mu = 0$. A and B are varied between 0 and 1 with 0.01 steps. The gray-scaled $M(M \leq 10)$ stands for the number of stably stored learning patterns. In the region of $(A + B/2) > 1$, the first few learning patterns ($\mu = 1, 2, 3$) are stable, but in the region of $(A + B/2) < 1$, the last few learning patterns ($\mu = 8, 9, 10$) are stable. The result is successfully explained by equation (10).

Fig. 3. The basin volume for each learning pattern ($\mu = 1, 2, \dots, 10$) obtained by Monte-Carlo simulation with 1000 randomly chosen initial conditions. The parameters are $A = 0.9$ and $C = 1.0$. The index μ is written at the curve which corresponds to the recency or the primacy effect.

Fig. 4. Formation of the basin for the 10 random learning patterns with the constraint $\sum_{j=1}^N \xi_j^\mu = 0$ after sleep; $p = 10$ and $l = 1000$. A and B are varied between 0 and 1 with 0.01 steps. All learning patterns are only stably stored around the line $(A + B/2) = 1$ which is consistent with equation (13). In the region of $(A + B/2) < 1$, memories for all learning patterns were completely washed out by sleep and in the region of $(A + B/2) > 1$, the first few learning patterns ($\mu = 1, 2, 3$) remain very strongly even after a long sleep.

Fig. 5. The basin volume for each learning pattern after sleep; $p = 10$ and $l = 1000$. The basin volume for the first few learning patterns increases very sharply when the value of B increases. This implies reinforcement of the primacy effect by sleep. The parameters are $A = 0.9$ and $C = 1.0$. The index μ is written at the curve which corresponds to the primacy effect.

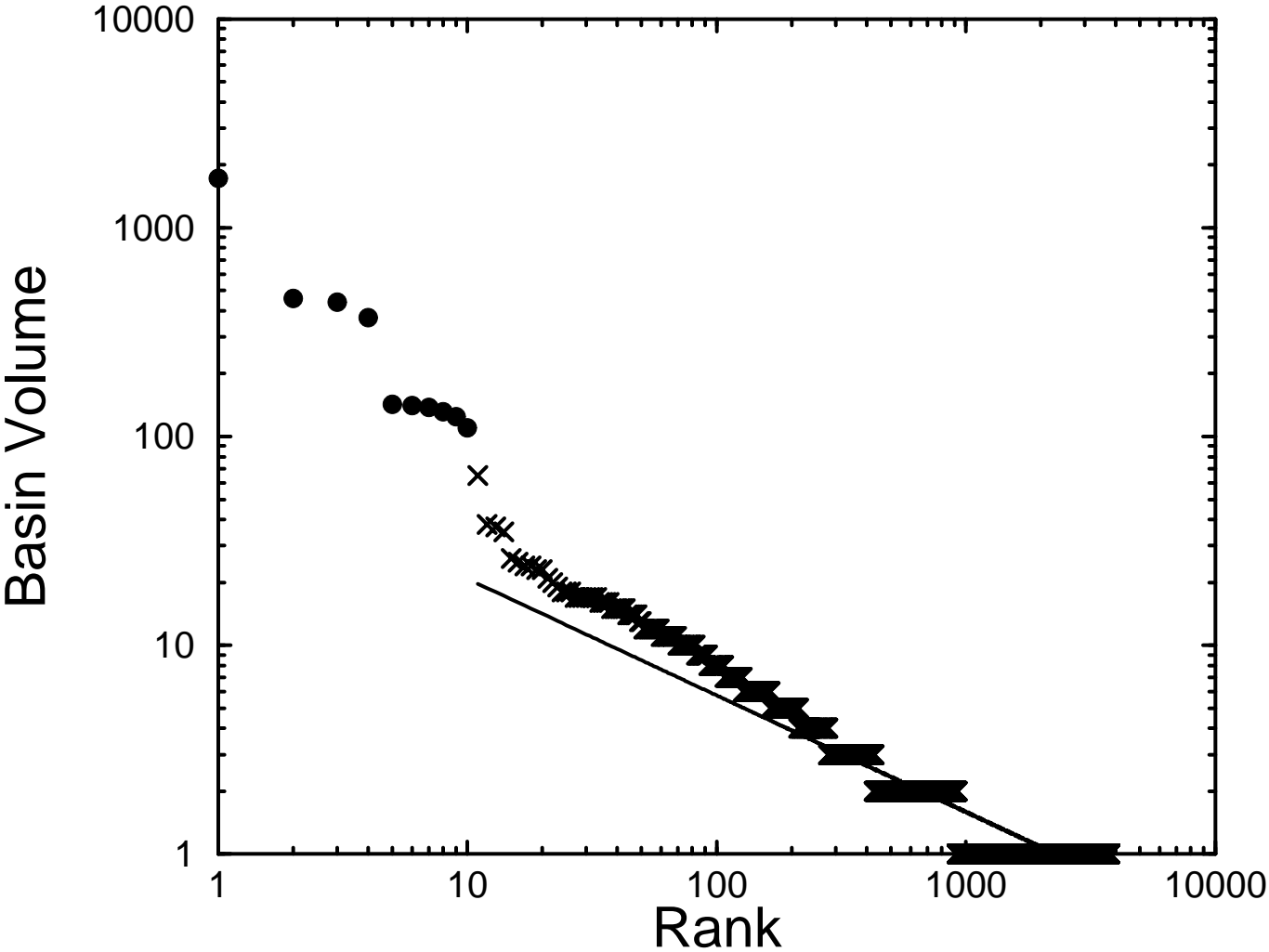
Fig. 6. The rank-size relation of Case 2 for the basin volume obtained by Monte-Carlo simulation with 10000 randomly chosen initial conditions. The parameters are $A = 1.0$, $B = 0.0$ and $C = 1.0$. The filled circles correspond to the learning patterns and the crosses to spurious states. The solid line is the fit of the spurious states by the least-squares method and the slope is -0.5582152 . This figure is the same as Figure 1 because the matrix element $w_{ij}(p)$ of equations (10) and (12) becomes equal for $B = 0$.

Fig. 7. Formation of the basin for the 10 random learning patterns. A and B are varied between 0 and 1 with 0.01 steps. In the region of $(A + B) > 1$, only the first learning pattern ($\mu = 1$) is stable, but in the region of $(A + B) < 1$, all learning patterns are stably stored at $A \approx 1$ and decrease as A decreases. The result is explained qualitatively well by equation (12).

Fig. 8. The basin volume for each learning pattern ($\mu = 1, 2, \dots, 10$) obtained by Monte-Carlo simulation with 1000 randomly chosen initial conditions. The parameters are $A = 0.9$ and $C = 1.0$. The index μ is written at the curve which corresponds to the recency or the primacy effect.

Fig. 9. Formation of the basin for the 10 random learning patterns after sleep; $p = 10$ and $l = 1000$. A and B are varied between 0 and 1 with 0.01 steps. In the region of $(A + B) < 1$, memories for all learning patterns were completely washed out by sleep and in the region of $(A + B) > 1$, the first learning pattern ($\mu = 1$) remains very strong even after a long sleep.

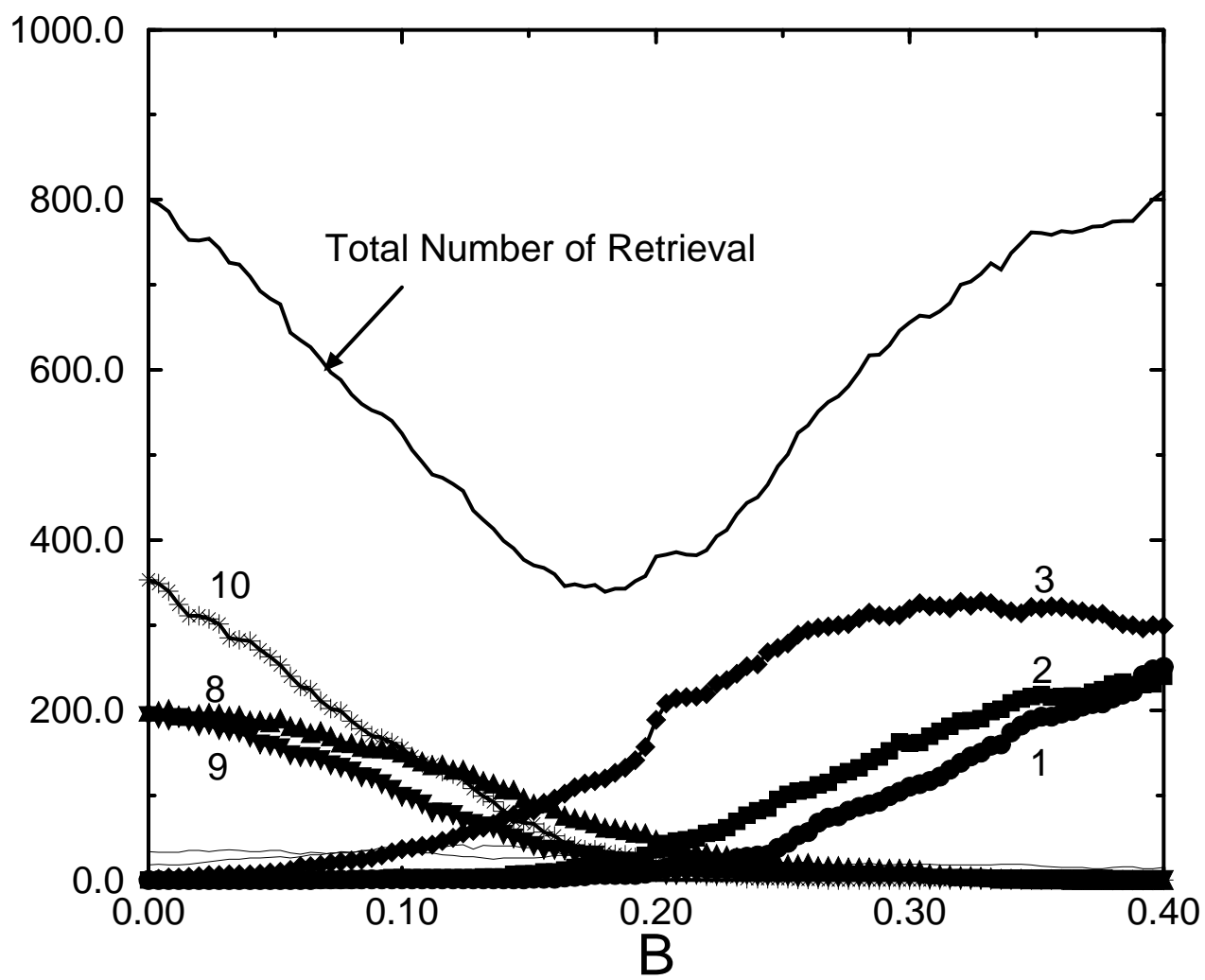
Fig. 10. The basin volume for the 10 learning patterns after sleep; $p = 10$ and $l = 1000$. The basin volume for the first learning pattern increases very sharply when the value of B increases. This implies reinforcement of the primacy effect by sleep. The parameters are $A = 0.9$ and $C = 1.0$. The index μ is written at the curve which corresponds to the primacy effect.



This figure "fig02.gif" is available in "gif" format from:

<http://arxiv.org/ps/cond-mat/9703212v1>

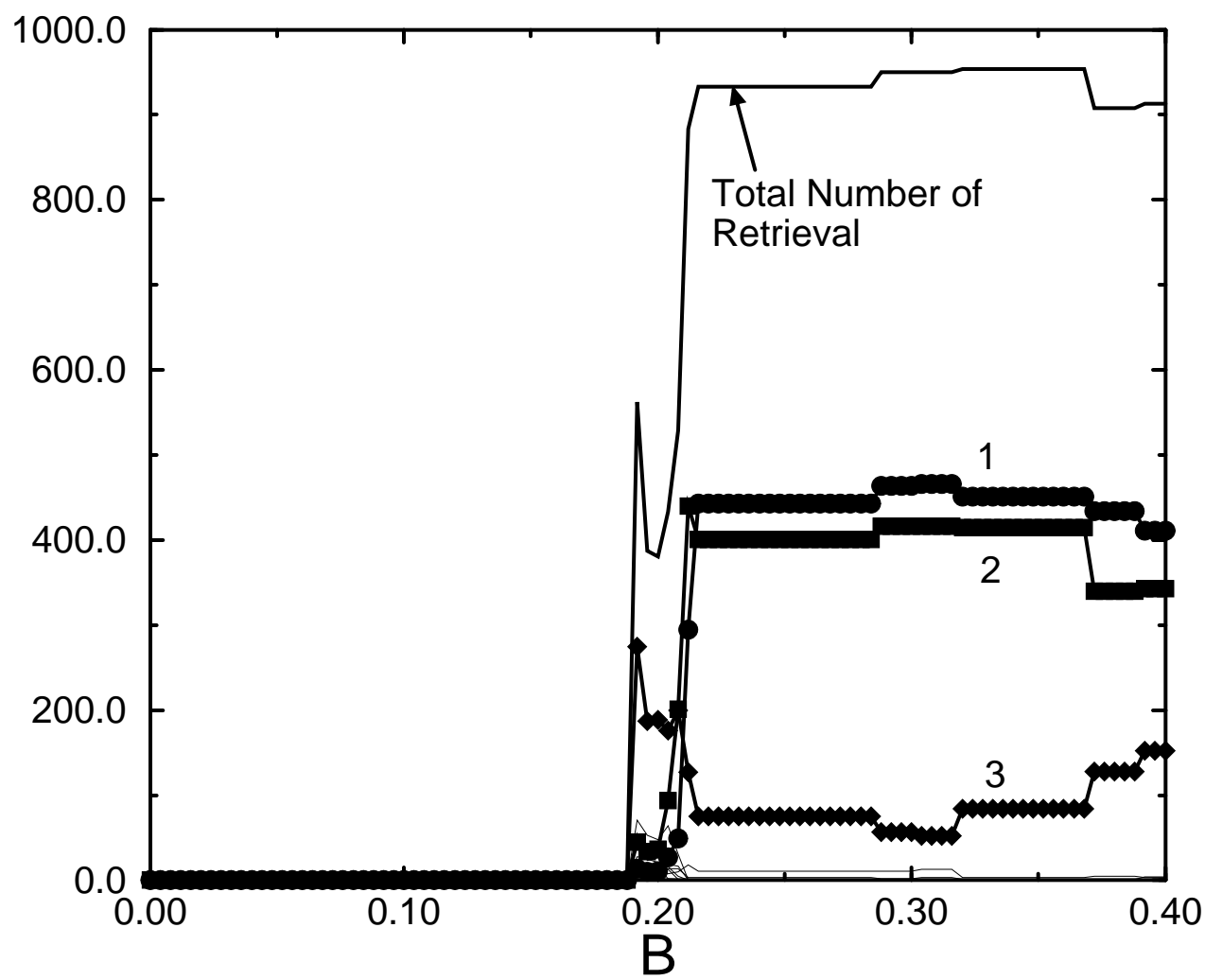
Basin Volume

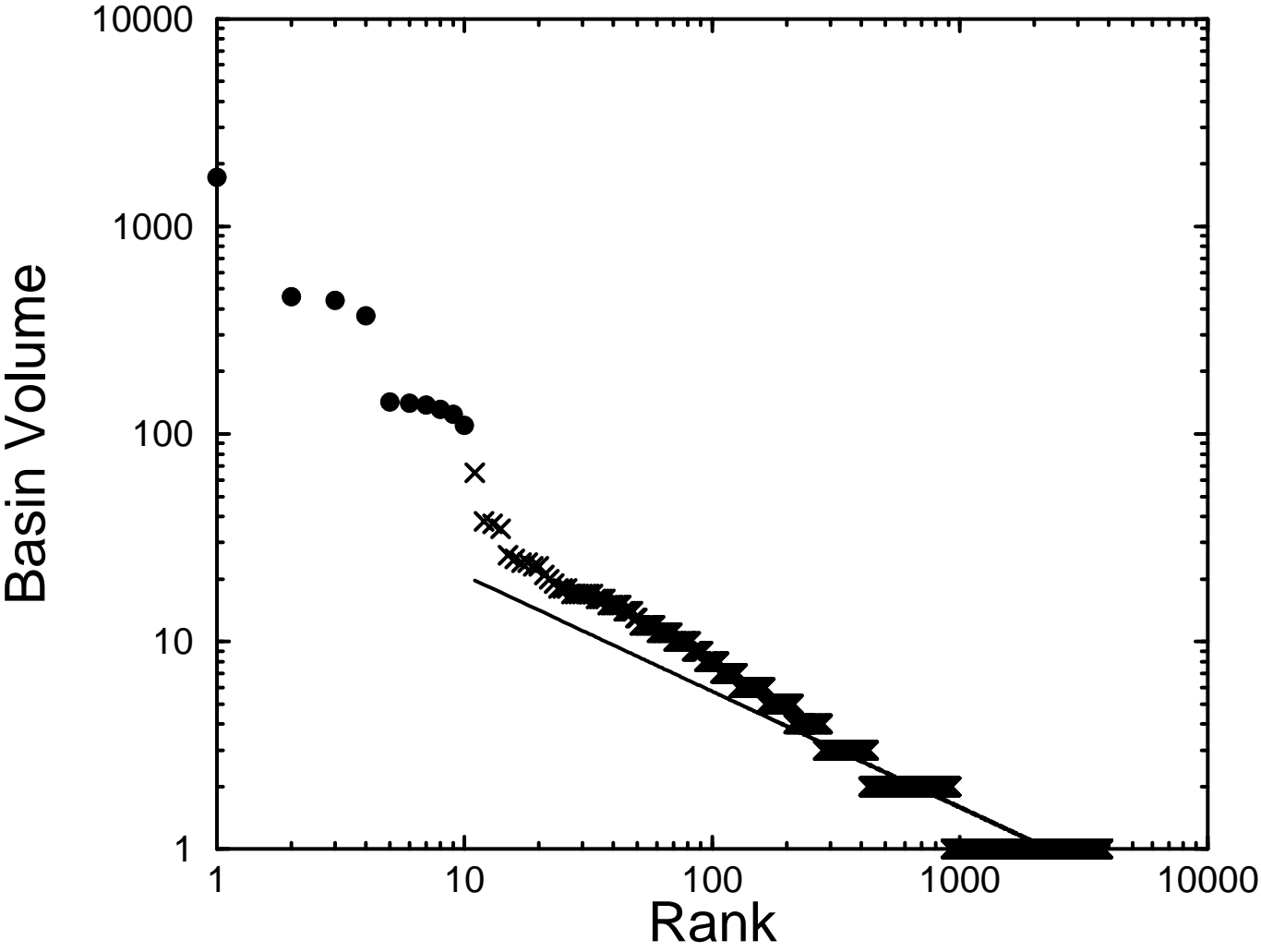


This figure "fig04.gif" is available in "gif" format from:

<http://arxiv.org/ps/cond-mat/9703212v1>

Basin Volume

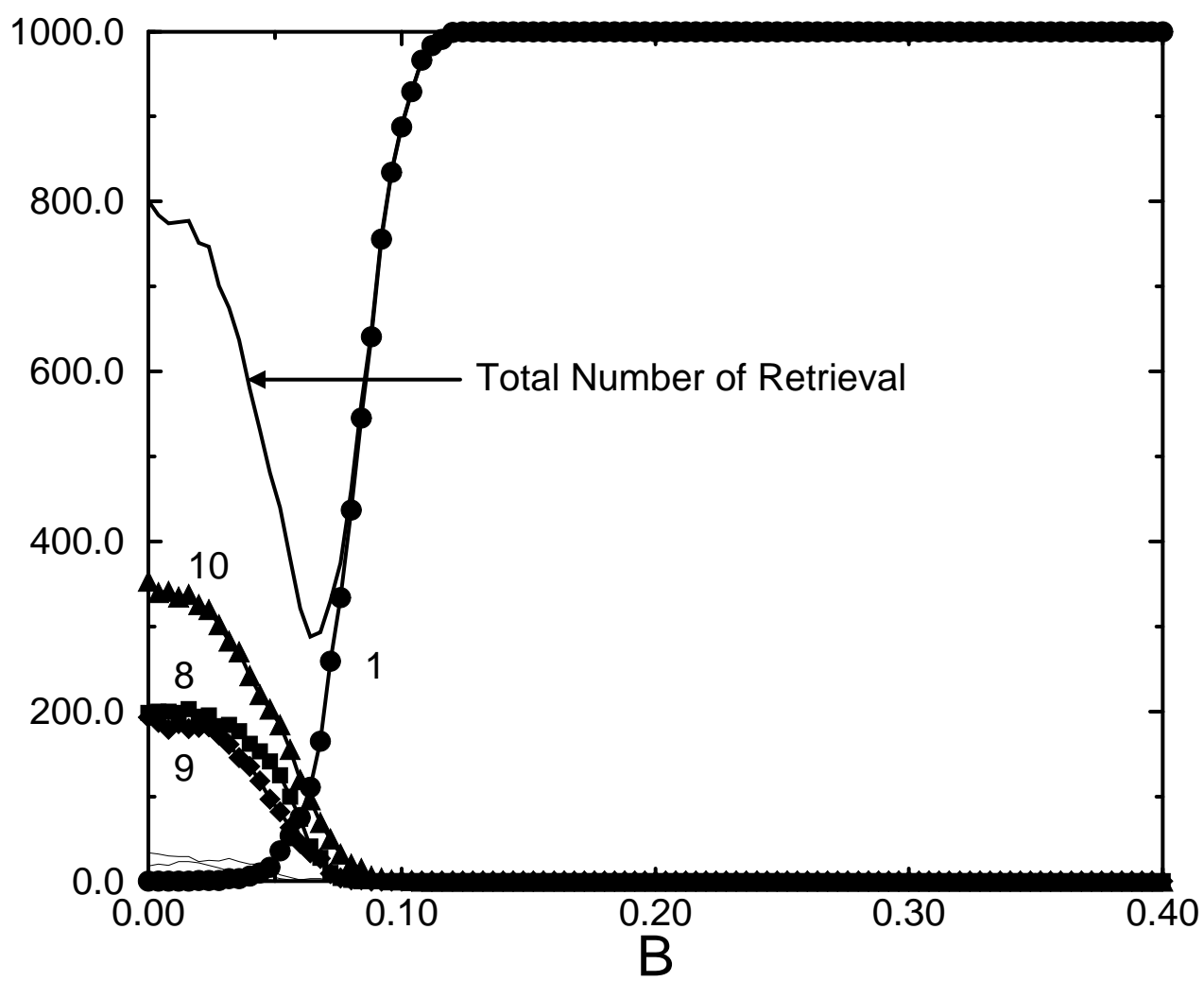




This figure "fig07.gif" is available in "gif" format from:

<http://arxiv.org/ps/cond-mat/9703212v1>

Basin Volume



This figure "fig09.gif" is available in "gif" format from:

<http://arxiv.org/ps/cond-mat/9703212v1>

